Atmos. Chem. Phys. Discuss., 15, 31153–31196, 2015
www.atmos-chem-phys-discuss.net/15/31153/2015/
doi:10.5194/acpd-15-31153-2015

Atmospheric Chemistry and Physics Discussions
Open Access

Role of methyl group number on SOA formation from aromatic hydrocarbons photooxidation under low NO_x conditions

L. Li[1,2], P. Tang[1,2], S. Nakao[1,2,a], C.-L. Chen[1,2,b], and D. R. Cocker III[1,2]

[1]University of California, Riverside, Department of Chemical and Environmental Engineering, Riverside, CA 92507, USA
[2]College of Engineering-Center for Environmental Research and Technology (CE-CERT), Riverside, CA 92507, USA
[a]currently at: Clarkson University, Department of Chemical and Biomolecular Engineering, Potsdam, NY 13699, USA
[b]currently at: Scripps Institution of Oceanography, University of California, La Jolla, California, USA

Received: 30 September 2015 – Accepted: 22 October 2015 – Published: 6 November 2015

Correspondence to: D. R. Cocker III (dcocker@engr.ucr.edu)

Published by Copernicus Publications on behalf of the European Geosciences Union.

Abstract

Substitution of methyl groups onto the aromatic ring determines the SOA formation from the aromatic hydrocarbon precursor. This study links the number of methyl groups on the aromatic ring to SOA formation from aromatic hydrocarbons photooxidation under low NO_x conditions (HC/NO > 10 ppbC : ppb). Aromatic hydrocarbons with increasing numbers of methyl groups are systematically studied. SOA formation from pentamethylbenzene and hexamethylbenzene are reported for the first time. A decreasing SOA yield with increasing number of methyl groups is observed. Linear trends are found in both f_{44} vs. f_{43} and O/C vs. H/C for SOA from aromatic hydrocarbons with zero to six methyl groups. An SOA oxidation state predictive method based on benzene is used to examine the effect of added methyl groups on aromatic oxidation under low NO_x conditions. Further, the impact of methyl group number on density and volatility of SOA from aromatic hydrocarbons is explored. Finally, a mechanism for methyl group impact on SOA formation is suggested. Overall, this work suggests as more methyl groups are attached on the aromatic ring, SOA products from these aromatic hydrocarbons become less oxidized per mass/carbon.

1 Introduction

Aromatic hydrocarbons are major anthropogenic SOA precursors (Kanakidou et al., 2005; Henze et al., 2008). Aromatic hydrocarbons with less than four methyl groups are ubiquitous in the atmosphere (Singh et al., 1985, 1992; Fraser et al., 1998; Pilling and Bartle, 1999; Holzinger et al., 2001; Buczynska et al., 2009; Hu et al., 2015). Aromatic hydrocarbons with more than 4 methyl groups are barely investigated in previous ambient studies, possibly due to a vapor pressure decrease with carbon number (Pankow and Asher, 2008; Table S1 in the Supplement). However, a recent study observed that compounds with low vapor pressure are available to evaporate into the atmosphere (Vǒ and Morris, 2012). Moreover, hydrocarbon reactivity and OH reaction rate constant (k_{OH}) increase with methyl group number (k_{OH} Table S1; Glasson et al., 1970; Calvert et al., 2002; Atkinson and Arey, 2003; Aschmann et al., 2013). OH-initiated reactions, particularly OH addition to the aromatic ring, dominate aromatic photooxidation (Calvert et al., 2002). Hence, photooxidation occurs rapidly once these low vapor pressure aromatic hydrocarbons evaporate into atmosphere. In addition, an increase in carbon number is associated with a decrease in vapor pressure (Pankow and Asher, 2008). Higher carbon number products with a similar amount of functional groups have a higher tendency to participate in the particle phase. However, aging of organic aerosol is a combination of functionalization, fragmentation and oligomerization (Jimenez et al., 2009; Kroll et al., 2009). Therefore, rapid aging does not necessarily lead to the highly oxidized compounds, which serve as an important source of SOA.

Recent studies have found that SOA yields from OH initiated alkane and alkene reactions increase with carbon chain length and decrease with methyl group branching ratio (Lim and Ziemann, 2009; Matsunaga et al., 2009; Tkacik et al., 2012). However, SOA yield from aromatics are found to decrease with carbon number by adding methyl groups to the aromatic ring (Odum et al., 1997; Cocker et al., 2001b; Sato et al., 2012). This indicates that the role of methyl groups on the aromatic ring is different than for aliphatic hydrocarbons. Previous studies show that the relative methyl group position determines the alkoxyl radical ($RO^•$) fragmentation ratio in aliphatic hydrocarbon oxidation (Atkinson, 2007; Ziemann, 2011). Therefore, it is necessary to explore the impact of methyl groups on SOA formation during aromatic hydrocarbon oxidation.

Previous studies on SOA formation from aromatic hydrocarbon in the presence of NO_x have been conducted at high NO_x levels (e.g., Odum et al., 1997; Cocker et al., 2001b; Sato et al., 2012). Ng et al. (2007) observed that SOA yield decreases with increasing carbon number under high NO_x conditions and no trends were observed for no NO_x conditions. Reaction mechanisms vary for different NO_x conditions (e.g., Song et al., 2005; Kroll and Seinfeld, 2008) and thus impact SOA chemical composition. Therefore, it is necessary to investigate methyl group impact on urban SOA formation from aromatic hydrocarbon under more atmospherically relevant low NO_x conditions.

SOA budget underestimation of the urban environment is associated with mechanism uncertainty in aromatic hydrocarbon photooxidation and possibly missing aromatic hydrocarbon precursors (Henze et al., 2008; Hallquist et al., 2009). Previous chamber studies seldom investigate SOA formation from aromatic with more than 3 methyl groups (e.g. pentamethylbenzene and hexamethylbenzene). This study investigates SOA formation from the photooxidation of seven aromatic hydrocarbon (ranging from benzene to hexamethylbenzene) under the low NO_x (HC/NO > 10 ppbC : ppb) condition. The impact of methyl group number on SOA yield, chemical composition and other physical properties are demonstrated. Possible methyl group impact on aromatic ring oxidation, decomposition and subsequent oligomerization are discussed.

2 Method

2.1 Environmental chamber

All experiments were conducted in the UC Riverside/CE-CERT indoor dual 90 m^3 environmental chambers, which are described in detail elsewhere (Carter et al., 2005). All experiments were conducted at dry conditions (RH < 0.1 %), in the absence of inorganic seed aerosol and with temperature controlled to 27 ± 1 °C. Two movable top frames were slowly lowered during each experiment to maintain a slight positive differential pressure (~ 0.02″ H_2O) between the reactors and enclosure to minimize dilution and/or contamination of the reactors. 272 115 W Sylvania 350BL blacklights are used as light sources for photooxidation.

A known volume of high purity liquid hydrocarbon precursors (benzene Sigma-Aldrich, 99 %; toluene Sigma-Aldrich, 99.5 %; *m*-xylene Sigma-Aldrich, 99 %; 1, 2, 4-trimethylbenzene Sigma-Aldrich, 98 %) were injected through a heated glass injection manifold system and flushed into the chamber with pure N_2. A glass manifold packed with glass wool inside a temperature controlled oven (50–80 °C) is used to inject solid hydrocarbon precursors (1, 2, 4, 5-tetramethylbenzene Sigma-Aldrich, 98 %;

pentamethylbenzene Sigma-Aldrich, 98 %; hexamethylbenzene Sigma-Aldrich, 99 %). NO was introduced by flushing pure N_2 through a calibrated glass bulb filled to a predetermined partial pressure of pure NO. All hydrocarbons and NO are injected and well mixed before the lights were turned on to commence the reaction.

2.2 Particle and gas measurement

Particle size distribution between 27 and 686 nm was monitored by dual custom built Scanning Mobility Particle Sizers (SMPS) (Cocker et al., 2001a). Particle effective density was measured with a Kanomax Aerosol Particle Mass Analyzer (APM-SMPS) system (Malloy et al., 2009). Particle volatility was measured by a Volatility Tandem Differential Mobility Analyzer (VTDMA) (Rader and McMurry, 1986) with a Dekati® Thermodenuder controlled to 100 °C and a 17 s heating zone residence time (Qi et al., 2010b). Volume remaining fraction (VRF) is calculated as $(D_{p,\text{ after TD}}/D_{p,\text{ before TD}})^3$.

Evolution of particle-phase chemical composition was measured by a High Resolution Time of Flight Aerosol Mass Spectrometer (HR-ToF-AMS; Aerodyne Research Inc.) (Canagaratna et al., 2007; DeCarlo et al., 2006). The sample was vaporized by a 600 °C oven followed by a 70 eV electron impact ionization. f_x in this study is calculated as the fraction of the organic signal at $m/z = x$. For example, f_{44} and f_{43} are the ratios of the organic signal at m/z 44 and 43 to the total organic signal, respectively (Chhabra et al., 2011; Duplissy et al., 2011). Elemental ratios for total organic mass, oxygen to carbon (O/C), and hydrogen to carbon (H/C) were determined using the elemental analysis (EA) technique (Aiken et al., 2007, 2008). Data was analyzed with ToF-AMS analysis toolkit squirrel 1.56D/PIKA 1.15D version.

The Agilent 6890 Gas Chromatograph – Flame Ionization Detector was used to measure aromatic hydrocarbon concentrations. A Thermal Environmental Instruments Model 42C chemiluminescence NO analyzer was used to monitor NO, NO_y-NO and NO_y. The gas-phase reaction model SAPRC-11 developed by Carter and Heo (2012) was utilized to predict radical concentrations ($^{\bullet}OH$, $HO_2^{\bullet}$, $RO_2^{\bullet}$ and $NO_3^{\bullet}$).

Discussion Paper | Discussion Paper | Discussion Paper | Discussion Paper |
ACPD
15, 31153–31196, 2015
Role of methyl group number on SOA formation
L. Li et al.

3 Results

3.1 SOA yield relationship with methyl group number

SOA yields from the photooxidation of six aromatic hydrocarbons are calculated as the mass based ratio of aerosol formed to hydrocarbon reacted (Odum et al., 1996). The HC/NO ratio ranged from 12.6–110 ppbC : ppb for all experiments used in this study. Experiment conditions and SOA yield are listed from the current work (Table 1) along with additional *m*-xylene experiment conditions from previous studies (Table 2) (Song et al., 2005) in the UCR CE-CERT chambers. SOA yield as a function of particle mass concentration (M_0) for all six aromatic precursors (Fig. 1) includes experiments listed in both Tables 1 and S2. Each individual experiment is marked and colored by the number of methyl groups on each precursor aromatic ring. It is observed that SOA yield decreases as the number of methyl groups increases (Fig. 1). A similar yield trend is also observed in previous studies on SOA formation from aromatic hydrocarbons, however, different absolute yield values are found, presumably due to higher NO_x levels (Odum et al., 1997b; Kleindienst et al., 1999; Cocker et al., 2001b; Takekawa et al., 2003; Ng et al., 2007; Sato et al., 2012). SOA yields of benzene under comparable low NO_x conditions are higher than that in Sato et al.(2012), Borrás and Tortajada-Genaro (2012) and Martín-Reviejo and Wirtz (2005).

The two product semi-empirical model described by Odum et al. (1996) is used to fit SOA yield as a function of M_0. Briefly, the two product model assumes that aerosol forming products can be lumped into lower and higher volatility groups whose mass fraction is defined by α_i and a partitioning parameter $K_{om,\,i}$ ($m^3\,\mu g^{-1}$) described extensively in Odum et al. (1996). Each aromatic hydrocarbon is fitted individually except for those with methyl group number greater than or equal to 4, which are grouped as C_{10+}. The experimental fitting parameters (α_1, $K_{om,\,1}$, α_2 and $K_{om,\,2}$ in Table 2) in the two product model were determined by minimizing the sum of the squared of the residuals. The more volatile parameters ($K_{om,\,2}$) are similar for all yield curve fits, suggesting that compounds of similar gas-particle partitioning parameters are formed from

ACPD
15, 31153–31196, 2015

the photooxidation of all aromatic hydrocarbons studied. Benzene has much higher mass-based stoichiometric coefficients (α_2) than the other aromatic compounds indicating that the pathway leading to higher volatility products formation is favored. The lower volatility partitioning parameters ($K_{om, 1}$) vary widely for each aromatic yield fitting curve. Benzene has the lowest $K_{om, 1}$, toluene has the highest $K_{om, 1}$, and the rest of aromatics have similar mid-range $K_{om, 1}$ values. The extremely low $K_{om, 1}$ of benzene indicates that pathways associated with significant volatility decrease occur far less during benzene photooxidation than for aromatic compounds with methyl groups. Further, $K_{om, 1}$ is much lower in multi-methyl group aromatic hydrocarbons (with the exception of toluene) while α_1 decreases with methyl group number. This suggests that increasing methyl group number on the aromatic ring suppresses SOA formation therefore lowering the mass based aerosol yield. This indicates that aromatics with more methyl groups are less oxidized per mass since the methyl group carbon is not well oxidized compared with the ring carbon.

The aromatic SOA growth curves (particle concentration M_0 vs. hydrocarbon consumption ΔHC) under similar HC/NO_x are shown in Fig. S1. The slope of the growth curve is negatively correlated with the parent aromatics reaction rate (k_{OH}). This observation contrasts with a previous study that observed positive correlation between SOA formation rate and hydrocarbon reaction rate for systems where initial semivolatile products dominate gas-particle phase partitioning (Chan et al., 2007). The reverse relationship observation in this study indicates that the methyl group number effect is greater than the effect of increasing k_{OH}. There are three possibilities for the methyl group number effect: (1) the methyl group facilitates initial semivolatile products to react into more volatile compounds; (2) the methyl group prevents further generation semivolatile products formation by stereo-hindrance; (3) the methyl group increases hydrocarbon mass consumption more than particle mass formation.

The relationship between radical levels and SOA yield was also analyzed. Table S3 lists modeled individual average radical parameter while Table S4 lists the correlation between SOA yields and individual average radical concentrations. None of the radi-

ACPD
15, 31153–31196, 2015

cal parameters (e.g. $^{\bullet}OH/HO_2^{\bullet}$, $HO_2^{\bullet}/RO_2^{\bullet}$ etc.) is strongly correlated with SOA yield. Average OH radical concentration is the best correlated parameter, as k_{OH} varies with aromatic species and lower average OH concentrations are present with higher k_{OH}. Figure S2 shows the time evolution of [$^{\bullet}OH$], [$RO_2^{\bullet}$] and [$HO_2^{\bullet}$] for different aromatic precursors under similar initial aromatic and NO_x loadings. Higher [$^{\bullet}OH$] is observed for aromatic precursors with lower k_{OH} while peroxide radicals ([$RO_2^{\bullet}$] and [$HO_2^{\bullet}$]), which depend on both k_{OH} and [$^{\bullet}OH$], are similar for all precursors. This suggests that SOA mass yield is determined by precursor structure rather than gas-phase oxidation state since radical conditions for each aromatic hydrocarbon are comparable and [$RO_2^{\bullet}$] and [$HO_2^{\bullet}$] reactions are expected to determine SOA formation (Kroll and Seinfeld, 2008).

3.2 SOA chemical composition relationship with methyl group number

3.2.1 f_{44} vs. f_{43}

Organic peaks at m/z 43 and m/z 44 are key fragments from AMS measurement toward characterization of oxygenated compounds in organic aerosol (Ng et al., 2010, 2011). The f_{44} and f_{43} evolution during SOA formation from different aromatic hydrocarbon photooxidation is shown for low NO_x conditions (Fig. 2). Each marker type represents an individual aromatic hydrocarbon with the marker colored by photooxidation time (light to dark). The f_{44} and f_{43} range are comparable to previous chamber studies with slight shift due to differences in initial conditions (e.g. NO_x etc.) (Ng et al., 2010; Chhabra et al., 2011; Loza et al., 2012; Sato et al., 2012). SOA compositions from aromatic hydrocarbon photooxidation under low NO_x are in the LV-OOA and SV-OOA range of the f_{44} vs. f_{43} triangle (Ng et al., 2010) with those from benzene on the left side, toluene inside and other aromatics on the right side of the triangle confirming that laboratory SOA f_{44} vs. f_{43} is precursor dependent (Chhabra et al., 2011). Significant f_{44} and f_{43} evolution trend is observed for benzene and slightly for toluene and *m*-xylene.

In this work, average f_{44} and f_{43} are examined to demonstrate the methyl group impact on SOA chemical composition from aromatic hydrocarbons. Average f_{44} vs.

ACPD
15, 31153–31196, 2015

f_{43} is marked with the aromatic compound name in Fig. 2. Generally decreasing f_{44} and increasing f_{43} are observed with increasing number of methyl groups on the aromatic ring. Similar trends are also observed in previous studies (Ng et al., 2010; Chhabra et al., 2011; Sato et al., 2012). The f_{44} vs. f_{43} trend is quantified by linear curve fitting ($f_{44} = -0.58 f_{43} + 0.19$, $R_2 = 0.94$). f_{28} is assumed to be equal to f_{44} in the AMS frag Table of Unit Resolution Analysis based on ambient studies (Zhang et al., 2005; Takegawa et al., 2007) and CO^+/CO_2^+ ratio for SOA from aromatic oxidation is found around ∼ 1 (0.9–1.3) (Chhabra et al., 2011). The slope of ∼ 0.5 indicates that $2\Delta f_{44} = -\Delta f_{43}$ or $\Delta(f_{28} + f_{44}) = -\Delta f_{43}$ in SOA formed from aromatic hydrocarbons with different numbers of methyl groups. The CO_2^+ fragment ion at m/z 44 and $C_2H_3O^+$ fragment ion at m/z 43 are two major AMS fragmentation ions from aromatic secondary organic aerosol. No significant $C_3H_7^+$ is observed at m/z 43. CO_2^+ represents oxidized aerosol and is associated with carboxylic acids (Alfarra et al., 2004; Aiken et al., 2007; Takegawa et al., 2007; Canagaratna et al., 2015) while $C_2H_3O^+$ is associated with carbonyls (McLafferty and Turecek, 1993; Ng et al., 2011). The CO^+ fragment ion at m/z 28 can originate from carboxylic acid or alcohol (Canagaratna et al., 2015). The $\Delta(f_{28}+f_{44}) = -\Delta f_{43}$ relationship observed in this study imply that adding the methyl group to the aromatic ring changes SOA from CO_2^+ to $C_2H_3O^+$ implying a less oxidized SOA chemical composition in AMS mass fragments. While bicyclic hydrogen peroxides are considered to be the predominant species in aerosol phase from aromatic photooxidation (Johnson et al., 2004, 2005; Wyche et al., 2009; Birdsall et al., 2010; Birdsall and Elrod, 2011; Nakao et al., 2011), they are less likely to contribute to the CO_2^+ ion fragment. Possible mechanisms to produce SOA products that form the CO_2^+ fragments as well as produce $C_2H_3O^+$ fragments by adding methyl group are described in detail in Sect. 4.

3.2.2 H/C vs. O/C

Elemental analysis (Aiken et al., 2007, 2008) is used to elucidate SOA chemical composition and SOA formation mechanisms (Heald et al., 2010; Chhabra et al., 2011).

ACPD
15, 31153–31196, 2015

Figure 3a shows the H/C and O/C time evolution of average SOA formed from hydrocarbon photooxidation of various aromatics under low NO_x conditions (marked and colored similarly to Fig. 2). The H/C and O/C ranges are comparable to previous chamber studies with slight shift due to difference in initial conditions (e.g. NO_x etc.) (Chhabra et al., 2011; Loza et al., 2012; Sato et al., 2012). All data points are located in between slope = −1 and slope = −2 (Fig. 3a, lower left corner, zoom out panel). This suggests that SOA components from aromatic photooxidation contain both carbonyl (ketone or aldehyde) and acid (carbonyl acid and hydroxycarbonyl) like functional groups. These elemental ratios also confirm that SOA formed from aromatic hydrocarbon photooxidation under low NO_x are among the LV-OOA and SV-OOA regions (Ng et al., 2011). The elemental ratio evolution trend agrees with the f_{44} vs. f_{43} trend. This study concentrates on average H/C and O/C in order to demonstrate the methyl group impact on SOA chemical composition from aromatic hydrocarbons.

Average H/C and O/C location is marked (Fig. 3a) for each aromatic compound by name. It is observed that H/C and O/C from SOA formed from *m*-xylene, 1, 2, 4-trimethylbenzene and aromatics with more than three methyl groups are similarly distributed in H/C vs. O/C. A general decrease in O/C and an increase in H/C are noted as the number of methyl groups on the aromatic ring increase, which is consistent with other studies (Chhabra et al., 2011; Sato et al., 2012). The trend indicates that aromatics are less oxidized per carbon as the number of methyl groups increases, which can be attributed to less oxidation of the methyl groups compared to the aromatic ring carbons. The elemental ratio trends (O/C decreases and H/C increases as the number of methyl groups increases) are also consistent with the decreasing yield trends with increasing the number of methyl groups (Sect. 3.1), suggesting that SOA yield is dependent on SOA chemical composition. Further, the yield and O/C ratio agrees with recent findings that O/C ratio is well correlated to aerosol volatility (Sect. 3.3.2) (Cappa et al., 2012; Yu et al., 2014) thereby affecting the extent of gas to particle partitioning. The H/C vs. O/C trend linear curve (H/C = −1.34 O/C + 2.00, $R^2 = 0.95$) shows an approximately −1 slope with a *y* axis (H/C) intercept of 2. The

ACPD
15, 31153–31196, 2015

H/C vs. O/C trend slope observed in this work is similar to the toluene and *m*-xylene elemental ratio slope observed under high NO_x and H_2O_2 only conditions observed in Chhabra et al. (2011).

The Van Krevelen diagram can also be used to analyze the oxidation pathway from initial SOA precursor to final SOA chemical composition by comparing the initial H/C and O/C ratios from the precursor hydrocarbon to the final SOA H/C and O/C ratios. Figure 3b shows the aromatic precursor location on the left (texted with aromatic hydrocarbon name and colored by methyl group number) and average SOA chemical composition on the right. The SOA H/C increase in the final SOA chemical composition follows the initial aromatic precursor elemental ratio trend. A large O/C increase with a slight H/C increase is observed moving from precursor to SOA composition. SOA formation from hydroperoxide bicyclic compounds contributes to O/C increases without loss of H. The slight H/C increase might result from hydrolysis of ring opened product oligomerization (Jang and Kamens, 2001; Jang et al., 2002; Kalberer et al., 2004; Sato et al., 2012). A slight H/C decrease rather than increase is observed in the hexamethylbenzene data suggesting that the six methyl groups sterically inhibits certain reaction mechanism (e.g. hydrolysis) to obtain H.

3.2.3 OS_c and its prediction

O/C alone may not capture oxidative changes as a result of breaking and forming of bonds (Kroll et al., 2009). Oxidation state of carbon ($OS_c \approx 2\,O/C - H/C$) was introduced into aerosol phase component analysis by Kroll et al. (2011). It is considered to be a more accurate metric for describing oxidation in atmospheric organic aerosol (Ng et al., 2011; Canagaratna et al., 2015; Lambe et al., 2015) and therefore better correlated with gas-particle partitioning (Aumont et al., 2012). Average SOA OS_c in this study ranges from −0.9 to 0.3 for aromatic photooxidation under low NO_x conditions (Fig. 4b) and is comparable to previous studies (Kroll et al., 2011, toluene, *m*-xylene and trimethylbenzene; Sato et al., 2012, benzene and 1,3,5-trimethylbenzene). OS_c observed is consistent with OS_c observed in field studies (Kroll et al., 2011) especially

ACPD
15, 31153–31196, 2015

in urban sites (e.g. −1.6 ~ 0.1, Mexico City) and supports the major role of aromatic precursors in producing anthropogenic aerosol. Average SOA OS_c values are consistent with the LV-OOA and SV-OOA regions (Ng et al., 2011; Kroll et al., 2011). OS_c only increases with oxidation time for benzene photooxidation (0.2 ~ 0.4).

The methyl group substitute ($-CH_3$) affects O/C and H/C ratios by increasing both carbon and hydrogen number as they relate to SOA OS_c. It is hypothesized here that the methyl group impacts remain similar in SOA elemental ratios as they do in the aromatic precursor ($-CH_3$ dilution effect). This would imply that the methyl group effect on SOA elemental ratio and OS_c from aromatic hydrocarbons is predictable from benzene oxidation. Equations (1) and (2) show the prediction formula for O/C and H/C, respectively, where i represents the methyl group number on the aromatic precursor, $O/C_{benzene\_SOA}$ and $H/C_{benzene\_SOA}$ are the measured O/C and H/C in SOA from benzene photooxidation experiments.

$$O/C_{pre,\,i} = \frac{6}{i+6}(O/C_{benzene\_SOA}) \quad (1)$$

$$H/C_{pre,\,i} = \frac{2i}{i+6} + \frac{6}{i+6}(H/C_{benzene\_SOA}) \quad (2)$$

Figure 4a shows a comparison of measured (red) and predicted (green) H/C and O/C location marked with corresponding SOA precursor methyl groups. The difference between predicted and measured H/C and O/C ranges from −6.4 ~ 1.2 % and −11.8 ~ 20.9 %, respectively. However, the predicted H/C vs. O/C line (Eqs. 1 and 2) is $H/C = -1.38\,O/C + 2.00$. This is comparable to a measured data fitting line (Sect. 3.2.2 $H/C = -1.34\,O/C + 2.00$, $R_2 = 0.95$). Predicted OS_c is then calculated based on the predicted H/C and O/C. Figure 4b compares measured (red) and predicted (green) OS_c. The largest O/C and OS_c overestimation is observed in *m*-xylene (marked as 2 in Fig. 4a, bar 2 in Fig. 4b). This could be explained by the isomer selected for the two methyl group aromatic hydrocarbon (*m*-xylene). A detailed analysis on isomer structure impact on SOA chemical composition is found in Li et al.(2015). The largest O/C and OS_c underestimation is observed in hexamethylbenzene (marked as 6 in Fig. 4a,

ACPD
15, 31153–31196, 2015

bar 6 in Fig. 4b). This suggests that the methyl groups attached to every aromatic carbon exert a steric inhibition effect on certain aromatic oxidation pathways, thus leading to increased importance of aerosol formation from other reaction pathways (possibly fragmentation Kroll et al., 2011, see Sect. 4) to form SOA.

The correlation between organic mass loading and chemical composition is also analyzed. Organic mass loading is well correlated (R^2) with chemical composition parameters including f_{44} (0.907), f_{43} (−0.910), H/C (−0.890) and O/C (0.923) (Fig. S3). However, previous studies show that O/C and f_{44} decrease as organic mass loading increases (Shilling et al., 2009; Ng et al., 2010; Pfaffenberger; 2013). The findings of this study indicate that molecular species drive SOA chemical composition rather than organic mass. The positive trend between f_{44} and organic mass loading is driven by benzene and toluene experiments (Fig. S3) where the high mass loading results are concurrent with high f_{44} results. However, the f_{44} change with mass loading increase during benzene and toluene photooxidation is less significant compared with the f_{44} difference caused by number of methyl groups on aromatic ring. Moreover, no significant correlation was found between mass loading and f_{44} or O/C when compared under similar mass loadings (including f_{44} at low mass loading time point of toluene and benzene photoxidation). Organic nitrate accounts for less than 10 % organic in SOA components in all aromatic hydrocarbon photooxidation experiments in this work according to AMS measurement and will not be discussed.

3.3 Physical property relationship with methyl group number

3.3.1 SOA density

SOA mass density is a fundamental parameter in understanding aerosol morphology, dynamics, phase and oxidation (De Carol et al., 2004; Katrib et al., 2005; Dinar et al., 2006; Cross et al., 2007). SOA density ranged from 1.24–1.44 $g\,cm^{-3}$ for all aromatic-NO_x photooxidation experiments in this study. The range is comparable to previous studies under similar conditions (Ng et al., 2007; Sato et al., 2010; Esther Borrás et al.,

ACPD
15, 31153–31196, 2015

2012). A general decreasing density trend is found with increasing methyl group number on precursor aromatic rings (see Fig. 5a). Correlation between SOA density and chemical composition was statistically analyzed (Table S5). Besides the strong correlation with methyl group number (−0.943, Fig. 5a), SOA density was also well correlated with O/C ratio (0.873, Fig. 5b) and other measures of bulk chemical composition (Table S5). Bahreini et al. (2005) reported a density increase trend with f_{44} in other compounds while Pang et al. (2006) found that SOA density increases with O/C ratio. Kuwata et al., 2011 (Eq. 3) and Nakao et al., 2013 suggested a quantified relationship between SOA density and SOA elemental ratio. Equation 3 developed by

$$\rho = \frac{12 + \mathrm{H/C} + 16 \times \mathrm{O/C}}{7 + 5 \times \mathrm{H/C} + 4.15 \times \mathrm{O/C}} \quad (3)$$

Kuwata et al. (2011) is used in this work to predict density based on elemental ratio in order to explore the methyl group impact on SOA formation. Figure 5c shows a good agreement between predicted and measured SOA densities (−6.58 % ~ 10.42 %). However, SOA density underestimation enlarges with increasing methyl group number (except hexamethylbenzene) implying that the increase of methyl groups promotes mechanism(s) leading to changes in the ratio of several key organic fragments (e.g., m/z 28: m/z 44) thereby challenging the applicability of the default fragment table for elemental ratio analysis. It is possible that CO^+/CO_2^+ and H_2O^+/CO_2^+ ratios are different in SOA formed from different aromatic precursors. Nakao et al. (2013) shows that H_2O^+/CO_2^+ increases with methyl group number due to the constant H_2O^+ fraction and a decrease in CO_2^+ fraction. Canagaratna et al.(2015) demonstrated that CO^+/CO_2^+ and H_2O^+/CO_2^+ are underestimated in certain compounds (especially alcohols). Assuming that the major impact of methyl group on SOA composition is to change –COOH to -$COCH_3$ (or other cyclic isomers), $f_{CO_2^+}$ will decrease but H_2O and CO^+ fraction might not change linearly. The alcohol contribution to CO^+/CO_2^+ and H_2O^+/CO_2^+ gradually grows as the methyl group prevents acid formation. Therefore, AMS measurements might underestimate O/C. This is consistent with the density prediction from elemental

ACPD
15, 31153–31196, 2015

ratios where a larger negative error is seen as the number of methyl groups increases, with the exception of hexamethylbenzene. This might relate to the difference in SOA formation pathways due to steric hindrance of the six methyl groups during hexamethylbenzene oxidation.

3.3.2 SOA volatility

SOA volatility is a function of oxidation, fragmentation, oligomerization and SOA mass (Kalberer et al., 2004; Salo et al., 2011; Tritscher et al., 2011; Yu et al., 2014). Bulk SOA volatility can be described by the VFR after heating SOA to a fixed temperature in a thermodenuder. VFRs for SOA formed early in the experiment are around 0.2 for all aromatic precursors and then increase as the experiment progresses. Increasing VFR indicates the gas to particle partitioning of more oxidized products, which may include oligomerization products formed during aromatic photooxidation. The VFR trends and ranges are comparable to previous studies (Kalberer et al., 2004; Qi et al., 2010a, b; Nakao et al., 2012). Figure 6a shows the relationship between SOA precursor methyl group number and SOA VFR at the end of the experiment (VFR_{end}). VFR shows a significant decreasing trend with increasing methyl group number from benzene to 1, 2, 4, 5-tetramethylbenzene. This implies that volatility of SOA-forming products increases as the number of methyl groups on the aromatic ring increases. There is also a slight increase in VFR from 1, 2, 4, 5-tetramethylbenzene to hexamethylbenzene; however, VFR in SOA formed from all C_{10+} group aromatics is lower than that of 1, 2, 4-trimethylbenzene. The changing VFR trend suggests that chemical components contributing to SOA formation become different when more than four methyl groups are attached to a single aromatic ring. A positive correlation (0.755, $p = 0.05$) found between mass loading and VFR_{end} implies that the lower the volatility in the products formed from aromatic hydrocarbons, the higher the SOA mass concentration. An opposite correlation between mass loading and VFR is found in previous studies due to the partitioning of more volatile compounds to the particle phase at high mass loading (Tritscher et al., 2011; Salo et al., 2011). Therefore, mass loading does not directly

ACPD
15, 31153–31196, 2015

lead to the VFR trend in the current study, rather it is the methyl group number in the SOA precursor that affects the composition of SOA and therefore the aromatic hydrocarbon yield (Sect. 3.1) and volatility. The correlation between SOA volatility (VFR) and chemical composition is statistically analyzed (Table S5). O/C (0.932, $p = 0.02$) and OS_c (0.931, $p = 0.02$) have the highest correlation with VFR_{end}. Previous studies also observed that lower aerosol volatility is correlated to higher O/C ratio (Cappa et al., 2012; Yu et al., 2014) and OS_c (Aumont et al., 2012; Hildebrandt Ruiz et al., 2014). Figure 6b and c illustrates the VFR_{end} and O/C or OS_c relationship among all the aromatic precursors investigated in this study. Benzene and toluene are located on the right upper corner in both graphs suggesting that significantly more oxidized and less volatile components are formed from aromatic precursors with less than two methyl groups. The VFR_{end} and chemical components relationship becomes less significant when only aromatic precursors with more than two methyl groups are considered.

4 Discussion

4.1 SOA formation pathway from aromatic hydrocarbon

Bicyclic peroxide compounds are considered to be important SOA forming products from aromatic photooxidation (Johnson et al., 2004, 2005; Song et al., 2005; Wyche et al., 2009; Birdsall et al., 2010; Birdsall and Elrod, 2011; Nakao et al., 2011). However, the significant CO_2^+ fragment (f_{44}) observed for SOA by the AMS indicates a contribution of an additional pathway to SOA formation from aromatic hydrocarbon photooxidation since it is unlikely that bicyclic peroxides could produce a CO_2^+ in the AMS. Hydrogen abstraction from the methyl group is not further discussed here as it accounts for less than 10 % aromatic oxidation pathway (Calvert et al., 2002). However, it is important to consider the further reaction of bicyclic peroxide ring scission products, especially in the presence of NO_x (Jang and Kamens, 2001; Atkinson and Arey, 2003; Song et al., 2005; Hu et al., 2007; Birdsall and Elrod, 2011; Carter et al., 2013). First

ACPD
15, 31153–31196, 2015

generation ring scission products include 1, 2-dicarbonyls (glyoxal and methylglyoxal) and unsaturated 1, 4-dicarbonyls (Forstner et al., 1997; Jang and Kamens, 2001; Birdsall and Elrod, 2011). These dicarbonyls are small volatile molecules that are unlikely to directly partition into the particle phase. However, these small molecules can potentially to grow into low volatility compounds through oligomerization. Previous studies suggest that oligomerization can be an important pathway for SOA formation from aromatic precursors (Edney et al., 2001; Baltensperger et al., 2005; Hu et al., 2007; Sato et al., 2012). While Kalberer et al.(2004) proposed an oligomerization pathway of 1, 2-dicarbonyls, Arey et al.(2008) found that unsaturated 1, 4-dicarbonyls have a higher molar yield than 1, 2-dicarbonyls in OH radical-initiated reaction of aromatic hydrocarbons. Further, OH radical reaction and photolysis rates are observed to be lower in 1, 2-dicarbonyls photolysis (Plum et al., 1983; Chen et al., 2000; Salter et al., 2013; Lockhart et al., 2013) than unsaturated 1, 4-dicarbonyls (Bierbach et al., 1994; Xiang et al., 2007). This suggests that secondary reaction of unsaturated 1, 4-dicarbonyls is more important than that of 1, 2-dicarbonyls. Previous studies have found that unsaturated 1, 4-dicarbonyls react to form small cyclic furanone compounds (Jang et al., 2001; Bloss et al., 2005; Aschmann et al., 2011). Oligomerization is possible for these small cyclic compounds based on their similar molecular structure with glyoxal and methylglyoxal (Fig. 7 c-2-1 and c-2-2 pathway, Fig. S4). Products from further oligomerization of ring opening compounds can also partition into the aerosol phase and contribute to SOA formation. Hydrolysis is necessary in both oligomerization pathways (Fig. S4 and Kalberer et al., 2004), which is consistent with the slight H/C increase observed for most aromatic hydrocarbon photooxidation results in this study. However, Nakao et al. (2012) showed that the glyoxal impact on SOA formation is majorly due to OH radical enhancement with glyoxal instead of oligomerization, especially under dry conditions. This indicates that oligomerization from small cyclic furanone is more likely to contribute more to SOA formation than 1, 2- dicarbonyl in this work. Other pathways reported in previous studies are also possible to contribute to SOA formation here (Edney et al., 2001, polyketone; Jang and Kamens, 2001, aromatic ring retaining products;

ACPD
15, 31153–31196, 2015

six and five member non-aromatic ring products; ring opening products; Bloss et al., 2005, benzoquinone, epoxide, phenol; Carter, 2013, bicyclic hydroperoxide). Our work only addresses differences in the oligomerization pathway contribution to form SOA from aromatic hydrocarbons.

A simplified aromatic oxidation mechanism for low NO_x conditions is shown (Figs. 7 and 8; the figures only illustrate aromatic oxidation related to particle formation). Figure 7 illustrates the oxidation, fragmentation and oligomerization after initial OH addition to aromatic ring, Fig. 8 shows the kinetic scheme for SOA formation from aromatic hydrocarbons. S_1, S_2 and S_3 represent bicyclic hydroperoxide compounds, ring opening compounds and oligomerization products, respectively. Table S6 summarizes the predicted vapor pressures of the benzene photooxidation products using SIMPOL (Pankow and Asher, 2008). The bicyclic hydroperoxide (S_1, Fig. 8) is more volatile than the oligomers (S_3 in Fig. 8). The volatilities of the bicyclic hydroperoxides are sufficiently high to allow additional oxidation (e.g. add one more hydroperoxide functional group to form $C_6H_6O_8$). The further oxidized bicyclic hydroperoxide vapor pressure is predicted to be similar to oligomerization products from reaction of c-2-1 (Fig. S4) with glyoxal. The higher vapor pressure of oligomer products from glyoxal as compared to oligomers from other products indicates that bicyclic hydroperoxides (S_1) contribute more to SOA formation in benzene than oligomerization products (S_2), as compared with aromatic hydrocarbons containing methyl groups according to the two product model fitting (Fig. 1 and Table 2).

4.2 Methyl group number impact on SOA formation pathway from aromatic hydrocarbon

It is observed that as the number of methyl groups on the aromatic precursor increases, mass yield (Sect. 3.1), overall oxidation per carbon (Sect. 3.2), and SOA density all decrease and SOA volatility increases. The observed yield trend is attributed to the increasing methyl group number enhancing aromatic fragmentation and inhibiting oligomerization. First, the methyl group stabilizes the ring opening radical (Atkinson,

ACPD
15, 31153–31196, 2015

2007; Ziemann, 2011), thus favoring the ring opening pathway. Second, the methyl group hinders cyclic compound formation and oligomerization (Fig. 7). Oligomerization is unlikely to occur directly from non-cyclic dicarbonyls (Kalberer et al., 2004) or indirectly from cyclic compounds formed by unsaturated dicarbonyls (Fig. S5) with increasing methyl group number. Methyl groups both inhibit oligomerization (Fig. 7, c-1-3) and prevent the formation of cyclic compounds from unsaturated dicarbonyls (Fig. 7, c-2-3) when methyl groups are attached to both ends of an unsaturated dicarbonyl. Hence, less cyclic compounds are available for subsequent oligomerization, leading to more volatile products and a decrease in SOA formation. Moreover, the SOA composition trend is well explained by a $-CH_3$ dilution effect. Previous studies on the different gas phase (Forstner et al., 1997; Yu et al., 1997) and particle phase (Hamilton et al., 2005; Sato et al., 2007, 2012) products supports this methyl group dilution theory. A typical example is that more 3-methyl-2,5-furandione is observed in *m*-xylene than toluene and vice versa for 2,5-furandione. Sato et al. (2010) suggests that more low-reactive ketones are produced rather than aldehydes with increasing number of substituents. However, most ketones or aldehydes detected are so volatile that they mostly exist in the gas phase (Forstner et al., 1997; Yu et al., 1997; Cocker et al., 2001b; Jang and Kamens, 2001). Taken collectively, this implies the importance of oligomerization and methyl substitutes on SOA formation.

The observation of a slight H/C decrease from hexamethylbenzene to its SOA components in contrast with the increasing trend for aromatic photooxidation for zero to five methyl group substitutes (Sect. 3.2.2) suggests that hydrolysis followed by oligomerization might not be significant when all aromatic ring carbons have attached methyl groups. Besides, the higher O/C and lower H/C (or the higher OS_c) than predicted in Sect. 3.2.3 indicates that SOA components from hexamethylbenzene photooxidation are more oxidized per carbon due to oxidation of the methyl groups, which is possibly related to the steric hindrance of the six methyl groups. Moreover, there is a slightly increasing trend in VFR from 1, 2, 4, 5-tetramethylbenzene to hexamethylbenzene (Sect. 3.3.2). Further studies (e.g. photooxidation using isotope labeled methyl group

ACPD
15, 31153–31196, 2015

hexamethylbenzene) are required to probe the unique SOA aspects from hexamethylbenzene photooxidation.

5 Atmospheric Implication

The impact of the number of methyl group substituents on SOA formation has been comprehensively studied in this work by integrating SOA yield with SOA chemical composition and SOA physical properties. A decreasing trend is found in the SOA mass yield and the carbon number averaged oxidation level with increasing number of methyl groups. SOA physical properties agree with yield and oxidation results. Therefore, this study demonstrates that the addition of methyl group substitutes to aromatic precursors decreases aromatic aging. Offsetting the amount of CO_2^+ and $C_2H_3O^+$ suggests a methyl group dilution effect on SOA formation from aromatic hydrocarbons. The proposed methyl group dilution effect is then applied successfully to the predict SOA elemental ratio. Overall, this study clearly demonstrates the methyl group impact on SOA formation from aromatic hydrocarbons.

Benzene and toluene are evaluated as the most important aromatic precursors to SOA formation among the six compounds studied due to their high SOA yields and highly oxidized components. Hexamethylbenzene is found to be significantly more oxidized than predicted based on other aromatic hydrocarbons studied here. This implies uniqueness in the methyl group behavior (no –H on aromatic ring) in hexamethylbenzene. Oligomerization is proposed to be an important pathway for SOA formation from aromatic hydrocarbons. It is likely that oligomerization is even more valuable to SOA formation from aromatic hydrocarbons under polluted areas (catalyzed effect, Jang et al., 2002; Iinuma et al., 2004; Noziere et al., 2008) and ambient humidity (Liggio et al., 2005a, b; Hastings et al., 2005).

ACPD
15, 31153–31196, 2015

The Supplement related to this article is available online at doi:10.5194/acpd-15-31153-2015-supplement.

Acknowledgements. We acknowledge funding support from National Science Foundation (ATM 0901282) and W. M. Keck Foundation. Any opinions, findings, and conclusions expressed in this material are those of the author(s) and do not necessarily reflect the views of the NSF.

References

Aiken, A. C., DeCarlo, P. F., and Jimenez, J. L.: Elemental analysis of organic species with electron ionization high-resolution mass spectrometry, Anal. Chem., 79, 8350–8358, doi:10.1021/ac071150w, 2007.

Aiken, A. C., DeCarlo, P. F., Kroll, J. H., Worsnop, D. R., Huffman, J. A., Docherty, K. S., Ulbrich, I. M., Mohr, C., Kimmel, J. R., Sueper, D., Sun, Y., Zhang, Q., Trimborn, A., Northway, M., Ziemann, P. J., Canagaratna, M. R., Onasch, T. B., Alfarra, M. R., Prevot, A. S. H., Dommen, J., Duplissy, J., Metzger, A., Baltensperger, U., and Jimenez, J. H.: O / C and OM / OC ratios of primary, secondary, and ambient organic aerosols with high-resolution time-of-flight aerosol mass spectrometry, Environ. Sci. Technol., 42, 4478–4485, doi:10.1021/es703009q, 2008.

Alfarra, M. R., Coe, H., Allan, J. D., Bower, K. N., Boudries, H., Canagaratna, M. R., Jimenez, J. L., Jayne, J. T., Garforth, A. A., Li, S. M., and Worsnop, D. R.: Characterization of urban and rural organic particulate in the lower Fraser valley using two aerodyne aerosol mass spectrometers, Atmos. Environ., 38, 5745–5758, doi:10.1016/j.atmosenv.2004.01.054, 2004.

Arey, J., Obermeyer, G., Aschmann, S. M., Chattopadhyay, S., Cusick, R. D., and Atkinson, R.: Dicarbonyl products of the OH radical-initiated reaction of a series of aromatic hydrocarbons, Environ. Sci. Technol., 43, 683–689, doi:10.1021/es8019098, 2008.

Aschmann, S. M., Nishino, N., Arey, J., and Atkinson, R.: Kinetics of the Reactions of OH Radicals with 2-and 3-Methylfuran, 2, 3-and 2, 5-Dimethylfuran, and E-and Z-3-Hexene-2, 5-dione, and Products of OH+ 2, 5-Dimethylfuran, Environ. Sci. Technol., 45, 1859–1865, doi:10.1021/es103207k, 2011.

Aschmann, S. M., Arey, J., and Atkinson, R.: Rate constants for the reactions of OH radicals with 1, 2, 4, 5-tetramethylbenzene, pentamethylbenzene, 2, 4, 5-trimethylbenzaldehyde, 2, 4, 5-trimethylphenol, and 3-methyl-3-hexene-2, 5-dione and products of OH+ 1, 2, 4, 5-tetramethylbenzene, J. Phys. Chem. A., 117, 2556–2568, doi:10.1021/jp400323n, 2013.

Atkinson, R.: Rate constants for the atmospheric reactions of alkoxy radicals: An updated estimation method, Atmos. Environ., 41, 8468–8485, doi:10.1016/j.atmosenv.2007.07.002, 2007.

Atkinson, R. and Arey, J.: Atmospheric degradation of volatile organic compounds, Chem. Rev., 103, 4605–4638, doi:10.1021/cr0206420, 2003.

Aumont, B., Valorso, R., Mouchel-Vallon, C., Camredon, M., Lee-Taylor, J., and Madronich, S.: Modeling SOA formation from the oxidation of intermediate volatility *n*-alkanes, Atmos. Chem. Phys., 12, 7577–7589, doi:10.5194/acp-12-7577-2012, 2012.

Bahreini, R., Keywood, M. D., Ng, N. L., Varutbangkul, V., Gao, S., Flagan, R. C., Seinfeld, J. H., Worsnop, D. R., and Jimenez, J. L.: Measurements of secondary organic aerosol from oxidation of cycloalkenes, terpenes, and *m*-xylene using an Aerodyne aerosol mass spectrometer, Environ. Sci. Technol., 39, 5674–5688, doi:10.1021/es048061a, 2005.

Baltensperger, U., Kalberer, M., Dommen, J., Paulsen, D., Alfarra, M. R., Coe, H., Fisseha, R., Gascho, A., Gysel, M., Nyeki, S., Sax, M., Steinbacher, M., Prevot, A. S. H., Sjögren, S., Weingartnera, E., and Zenobib, R.: Secondary organic aerosols from anthropogenic and biogenic precursors, Faraday. Discuss., 130, 265–278, doi:10.1039/b417367h, 2005.

Bierbach, A., Barnes, I., Becker, K. H., and Wiesen, E.: Atmospheric chemistry of unsaturated carbonyls: Butenedial, 4-oxo-2-pentenal, 3-hexene-2, 5-dione, maleic anhydride, 3H-furan-2-one, and 5-methyl-3H-furan-2-one, Environ. Sci. Technol., 28, 715–729, doi:10.1021/es00053a028, 1994.

Birdsall, A. W. and Elrod, M. J.: Comprehensive NO-dependent study of the products of the oxidation of atmospherically relevant aromatic compounds, J. Phys. Chem. A., 115, 5397–5407, doi:10.1021/jp2010327, 2011.

Birdsall, A. W., Andreoni, J. F., and Elrod, M. J.: Investigation of the role of bicyclic peroxy radicals in the oxidation mechanism of toluene, J. Phys. Chem. A., 114, 10655–10663, doi:10.1021/jp105467e, 2010.

Bloss, C., Wagner, V., Jenkin, M. E., Volkamer, R., Bloss, W. J., Lee, J. D., Heard, D. E., Wirtz, K., Martin-Reviejo, M., Rea, G., Wenger, J. C., and Pilling, M. J.: Development of a

detailed chemical mechanism (MCMv3.1) for the atmospheric oxidation of aromatic hydrocarbons, Atmos. Chem. Phys., 5, 641–664, doi:10.5194/acp-5-641-2005, 2005.
Borrás, E. and Tortajada-Genaro, L. A.: Secondary organic aerosol formation from the photo-oxidation of benzene, Atmos. Environ., 47, 154–163, doi:10.1016/j.atmosenv.2011.11.020, 2012.
Buczynska, A. J., Krata, A., Stranger, M., Godoi, A. F. L., Kontozova-Deutsch, V., Bencs, L., Naveau, I., Roekens, E., and Van Grieken, R.: Atmospheric BTEX-concentrations in an area with intensive street traffic, Atmos. Environ., 43, 311–318, doi:10.1016/j.atmosenv.2008.09.071, 2009.
Calvert, J. G., Atkinson, R., Becker, K. H., Kamens, R. M., Seinfeld, J. H., Wallington, T. J., and Yarwood, G.: The Mechanisms of Atmospheric Oxidation of Aromatic Hydrocarbons, Oxford University Press, New York, USA, 2002.
Canagaratna, M. R., Jayne, J. T., Jimenez, J. L., Allan, J. D., Alfarra, M. R., Zhang, Q., Onasch, T. B., Drewnick, F., Coe, H., Middlebrook, A., Delia, A., Williams, L. R., Trimborn, A. M., Northway, M. J., DeCarlo, P. F., Kolb, C. E., Davidovits, P., and Worsnop, D. R.: Chemical and microphysical characterization of ambient aerosols with the aerodyne aerosol mass spectrometer, Mass. Spectrom. Rev., 26, 185–222, doi:10.1002/mas.20115, 2007.
Canagaratna, M. R., Jimenez, J. L., Kroll, J. H., Chen, Q., Kessler, S. H., Massoli, P., Hildebrandt Ruiz, L., Fortner, E., Williams, L. R., Wilson, K. R., Surratt, J. D., Donahue, N. M., Jayne, J. T., and Worsnop, D. R.: Elemental ratio measurements of organic compounds using aerosol mass spectrometry: characterization, improved calibration, and implications, Atmos. Chem. Phys., 15, 253–272, doi:10.5194/acp-15-253-2015, 2015.
Cappa, C. D. and Wilson, K. R.: Multi-generation gas-phase oxidation, equilibrium partitioning, and the formation and evolution of secondary organic aerosol, Atmos. Chem. Phys., 12, 9505–9528, doi:10.5194/acp-12-9505-2012, 2012.
Carter, W. P. L. and Heo, G.: Development of Revised SAPRC Aromatics Mechanisms, California Air Resources Board, Sacramento, CA, USA, 2012.
Carter, W. P. L. and Heo, G.: Development of revised SAPRC aromatics mechanisms, Atmos. Environ., 77, 404–414, doi:10.1016/j.atmosenv.2013.05.021, 2013.
Carter, W. P. L., Cocker III, D. R., Fitz, D. R., Malkina, I. L., Bumiller, K., Sauer, C. G., Pisano, J. T., Bufalino, C., and Song, C.: A new environmental chamber for evaluation of gas-phase chemical mechanisms and secondary aerosol formation, Atmos. Environ., 39, 7768–7788, doi:10.1016/j.atmosenv.2005.08.040, 2005.

ACPD
15, 31153–31196, 2015

Role of methyl group number on SOA formation

L. Li et al.

Chan, A. W. H., Kroll, J. H., Ng, N. L., and Seinfeld, J. H.: Kinetic modeling of secondary organic aerosol formation: effects of particle-and gas-phase reactions of semivolatile products, Atmos. Chem. Phys., 7, 4135–4147, doi:10.5194/acp-7-4135-2007, 2007.
Chen, Y., Wang, W., and Zhu, L.: Wavelength-dependent photolysis of methylglyoxal in the 290–440 nm region, J. Phys. Chem. A., 104, 11126–11131, doi:10.1021/jp002262t, 2000.
Chhabra, P. S., Ng, N. L., Canagaratna, M. R., Corrigan, A. L., Russell, L. M., Worsnop, D. R., Flagan, R. C., and Seinfeld, J. H.: Elemental composition and oxidation of chamber organic aerosol, Atmos. Chem. Phys., 11, 8827–8845, doi:10.5194/acp-11-8827-2011, 2011.
Cocker III, D. R., Flagan, R. C., and Seinfeld, J. H.: State-of-the-art chamber facility for studying atmospheric aerosol chemistry, Environ. Sci. Technol., 35, 2594–2601, doi:10.1021/es0019169, 2001a.
Cocker III, D. R., Mader, B. T., Kalberer, M., Flagan, R. C., and Seinfeld, J. H.: The effect of water on gas–particle partitioning of secondary organic aerosol: II. *m*-xylene and 1, 3, 5-trimethylbenzene photooxidation systems, Atmos. Environ., 35, 6073–6085, doi:10.1016/S1352-2310(01)00405-8, 2001b.
Cross, E. S., Slowik, J. G., Davidovits, P., Allan, J. D., Worsnop, D. R., Jayne, J. T., Lewis, D. K., Canagaratna, M., and Onasch, T. B.: Laboratory and ambient particle density determinations using light scattering in conjunction with aerosol mass spectrometry, Aerosol Sci. Tech., 41, 343–359, doi:10.1080/02786820701199736, 2007.
DeCarlo, P. F., Slowik, J. G., Worsnop, D. R., Davidovits, P., and Jimenez, J. L.: Particle morphology and density characterization by combined mobility and aerodynamic diameter measurements, Part 1: Theory, Aerosol Sci. Tech., 38, 1185–1205, doi:10.1080/027868290903907, 2004.
DeCarlo, P. F., Kimmel, J. R., Trimborn, A., Northway, M. J., Jayne, J. T., Aiken, A. C., Gonin, M., Fuhrer, K., Horvath, T., Docherty, K. S., Worsnop, D. R., and Jimenez, J. L.: Field-deployable, high-resolution, time-of-flight aerosol mass spectrometer, Anal. Chem., 78, 8281–8289, doi:10.1021/ac061249n, 2006.
Dinar, E., Mentel, T. F., and Rudich, Y.: The density of humic acids and humic like substances (HULIS) from fresh and aged wood burning and pollution aerosol particles, Atmos. Chem. Phys., 6, 5213–5224, doi:10.5194/acp-6-5213-2006, 2006.
Duplissy, J., DeCarlo, P. F., Dommen, J., Alfarra, M. R., Metzger, A., Barmpadimos, I., Prevot, A. S. H., Weingartner, E., Tritscher, T., Gysel, M., Aiken, A. C., Jimenez, J. L., Canagaratna, M. R., Worsnop, D. R., Collins, D. R., Tomlinson, J., and Baltensperger, U.: Relating

hygroscopicity and composition of organic aerosol particulate matter, Atmos. Chem. Phys., 11, 1155–1165, doi:10.5194/acp-11-1155-2011, 2011.
Edney, E., Driscoll, D., Weathers, W., Kleindienst, T., Conver, T., McIver, C., and Li, W.: Formation of polyketones in irradiated toluene/propylene/NO_x/air mixtures, Aerosol Sci. Tech., 35, 998–1008, doi:10.1080/027868201753306769, 2001.
Forstner, H. J. L., Flagan, R. C., and Seinfeld, J. H.: Secondary organic aerosol from the photooxidation of aromatic hydrocarbons: Molecular composition, Environ. Sci. Technol., 31, 1345–1358, doi:10.1021/es9605376, 1997.
Fraser, M. P., Cass, G. R., Simoneit, B. R., and Rasmussen, R.: Air quality model evaluation data for organics. 5. C_6-C_{22} nonpolar and semipolar aromatic compounds, Environ. Sci. Technol., 32, 1760–1770, doi:10.1021/es970349v, 1998.
Glasson, W. A. and Tuesday, C. S.: Hydrocarbon reactivities in the atmospheric photooxidation of nitric oxide, Environ. Sci. Technol., 4, 916–924, doi:10.1021/es60046a002, 1970.
Hallquist, M., Wenger, J. C., Baltensperger, U., Rudich, Y., Simpson, D., Claeys, M., Dommen, J., Donahue, N. M., George, C., Goldstein, A. H., Hamilton, J. F., Herrmann, H., Hoffmann, T., Iinuma, Y., Jang, M., Jenkin, M. E., Jimenez, J. L., Kiendler-Scharr, A., Maenhaut, W., McFiggans, G., Mentel, Th. F., Monod, A., Prévôt, A. S. H., Seinfeld, J. H., Surratt, J. D., Szmigielski, R., and Wildt, J.: The formation, properties and impact of secondary organic aerosol: current and emerging issues, Atmos. Chem. Phys., 9, 5155–5236, doi:10.5194/acp-9-5155-2009, 2009.
Hamilton, J. F., Webb, P. J., Lewis, A. C., and Reviejo, M. M.: Quantifying small molecules in secondary organic aerosol formed during the photo-oxidation of toluene with hydroxyl radicals, Atmos. Environ., 39, 7263–7275, doi:10.1016/j.atmosenv.2005.09.006, 2005.
Hassoun, S., Pilling, M. J., and Bartle, K. D.: A catalogue of urban hydrocarbons for the city of Leeds: atmospheric monitoring of volatile organic compounds by thermal desorption-gas chromatography, J. Environ. Monitor., 1, 453–458, doi:10.1039/a904879k, 1999.
Hastings, W. P., Koehler, C. A., Bailey, E. L., and De Haan, D. O.: Secondary organic aerosol formation by glyoxal hydration and oligomer formation: Humidity effects and equilibrium shifts during analysis, Environ. Sci. Technol., 39, 8728–8735, doi:10.1021/es050446l, 2005.
Heald, C. L., Kroll, J. H., Jimenez, J. L., Docherty, K. S., DeCarlo, P. F., Aiken, A. C., Chen, Q., Martin, S. T., Farmer, D. K., and Artaxo, P.: A simplified description of the evolution of organic aerosol composition in the atmosphere, Geophys. Res. Lett., 37, L08803, doi:10.1029/2010GL042737, 2010.

Henze, D. K., Seinfeld, J. H., Ng, N. L., Kroll, J. H., Fu, T.-M., Jacob, D. J., and Heald, C. L.: Global modeling of secondary organic aerosol formation from aromatic hydrocarbons: high-vs. low-yield pathways, Atmos. Chem. Phys., 8, 2405–2420, doi:10.5194/acp-8-2405-2008, 2008.

Hildebrandt Ruiz, L., Paciga, A. L., Cerully, K., Nenes, A., Donahue, N. M., and Pandis, S. N.: Aging of secondary organic aerosol from small aromatic VOCs: changes in chemical composition, mass yield, volatility and hygroscopicity, Atmos. Chem. Phys. Discuss., 14, 31441–31481, doi:10.5194/acpd-14-31441-2014, 2014.

Holzinger, R., Kleiss, B., Donoso, L., and Sanhueza, E.: Aromatic hydrocarbons at urban, sub-urban, rural (8°52′ N; 67°19′ W) and remote sites in Venezuela, Atmos. Environ., 35, 4917–4927, doi:10.1016/S1352-2310(01)00286-2, 2001.

Hu, D. and Kamens, R. M.: Evaluation of the UNC toluene-SOA mechanism with respect to other chamber studies and key model parameters, Atmos. Environ., 41, 6465–6477, doi:10.1016/j.atmosenv.2007.04.026, 2007.

Hu, D., Tolocka, M., Li, Q., and Kamens, R. M.: A kinetic mechanism for predicting secondary organic aerosol formation from toluene oxidation in the presence of NO_x and natural sunlight, Atmos. Environ., 41, 6478–6496, doi:10.1016/j.atmosenv.2007.04.025, 2007.

Hu, L., Millet, D. B., Baasandorj, M., Griffis, T. J., Travis, K. R., Tessum, C. W., Marshall, J. D., Reinhart, W. F., Mikoviny, T., Müller, M., Wisthaler, A., Graus, M., Warneke, C., and de Gouw, J.: Emissions of C_6–C_8 aromatic compounds in the United States: Constraints from tall tower and aircraft measurements, J. Geophys. Res.-Atmos., 120, 826–842, doi:10.1002/2014JD022627, 2015.

Iinuma, Y., Böge, O., Gnauk, T., and Herrmann, H.: Aerosol-chamber study of the α-pinene/O_3 reaction: influence of particle acidity on aerosol yields and products, Atmos. Environ., 38, 761–773, doi:10.1016/j.atmosenv.2003.10.015, 2004.

Jang, M. and Kamens, R. M.: Characterization of secondary aerosol from the photooxidation of toluene in the presence of NO_x and 1-propene, Environ. Sci. Technol., 35, 3626–3639, doi:10.1021/es010676+, 2001.

Jang, M., Czoschke, N. M., Lee, S., and Kamens, R. M.: Heterogeneous atmospheric aerosol production by acid-catalyzed particle-phase reactions, Science, 298, 814–817, doi:10.1126/science.1075798, 2002.

Jimenez, J. L., Canagaratna, M. R., Donahue, N. M., Prevot, A. S. H., Zhang, Q., Kroll, J. H., DeCarlo, P. F., Allan, J. D., Coe, H., Ng, N. L., Aiken, A. C., Docherty, K. S., Ulbrich, I. M., Grieshop, A. P., Robinson, A. L., Duplissy, J., Smith, J. D., Wilson, K. R., Lanz, V. A., Hueglin, C., Sun, Y. L., Tian, J., Laaksonen, A., Raatikainen, T., Rautiainen, J., Vaattovaara, P., Ehn, M., Kulmala, M., Tomlinson, J. M., Collins, D. R., Cubison, M. J., Dunlea1, E., J., Huffman, J. A., Onasch, T. B., Alfarra, M. R., Williams, P. I., Bower, K., Kondo, Y., Schneider, J., Drewnick, F., Borrmann, S., Weimer, S., Demerjian, K., Salcedo, D., Cottrell, L., Griffin, R., Takami, A., Miyoshi, T., Hatakeyama, S., Shimono, A., Sun, J. Y., Zhang, Y. M., Dzepina, K., Kimmel, J. R., Sueper, D., J. Jayne, T., Herndon, S. C., Trimborn, A. M., Williams, L. R., Wood, E. C., Middlebrook, A. M., Kolb, C. E., Baltensperger, U., and Worsnop, D. R.: Evolution of organic aerosols in the atmosphere, Science, 326, 1525–1529, doi:10.1126/science.1180353, 2009.

Johnson, D., Jenkin, M. E., Wirtz, K., and Martin-Reviejo, M.: Simulating the formation of secondary organic aerosol from the photooxidation of toluene, Environ. Chem., 1, 150–165, doi:10.1071/EN04069, 2004.

Johnson, D., Jenkin, M. E., Wirtz, K., and Martin-Reviejo, M.: Simulating the formation of secondary organic aerosol from the photooxidation of aromatic hydrocarbons, Environ. Chem., 2, 35–48, doi:10.1071/EN04079, 2005.

Kalberer, M., Paulsen, D., Sax, M., Steinbacher, M., Dommen, J., Prevot, A. S. H., Fisseha, R., Weingartner, E., Frankevich, V., and Zenobi, R.: Identification of polymers as major components of atmospheric organic aerosols, Science, 303, 1659–1662, doi:10.1126/science.1092185, 2004.

Kanakidou, M., Seinfeld, J. H., Pandis, S. N., Barnes, I., Dentener, F. J., Facchini, M. C., Van Dingenen, R., Ervens, B., Nenes, A., Nielsen, C. J., Swietlicki, E., Putaud, J. P., Balkanski, Y., Fuzzi, S., Horth, J., Moortgat, G. K., Winterhalter, R., Myhre, C. E. L., Tsigaridis, K., Vignati, E., Stephanou, E. G., and Wilson, J.: Organic aerosol and global climate modelling: a review, Atmos. Chem. Phys., 5, 1053–1123, doi:10.5194/acp-5-1053-2005, 2005.

Katrib, Y., Martin, S. T., Rudich, Y., Davidovits, P., Jayne, J. T., and Worsnop, D. R.: Density changes of aerosol particles as a result of chemical reaction, Atmos. Chem. Phys., 5, 275–291, doi:10.5194/acp-5-275-2005, 2005.

Kleindienst, T. E., Smith, D. F., Li, W., Edney, E. O., Driscoll, D. J., Speer, R. E., and Weathers, W. S.: Secondary organic aerosol formation from the oxidation of aromatic hydrocarbons in the presence of dry submicron ammonium sulfate aerosol, Atmos. Environ., 33, 3669–3681, doi:10.1016/S1352-2310(99)00121-1, 1999.

ACPD
15, 31153–31196, 2015

Kroll, J. H. and Seinfeld, J. H.: Chemistry of secondary organic aerosol: Formation and evolution of low-volatility organics in the atmosphere, Atmos. Environ., 42, 3593–3624, doi:10.1016/j.atmosenv.2008.01.003, 2008.

Kroll, J. H., Smith, J. D., Che, D. L., Kessler, S. H., Worsnop, D. R., and Wilson, K. R.: Measurement of fragmentation and functionalization pathways in the heterogeneous oxidation of oxidized organic aerosol, Phys. Chem. Chem. Phys., 11, 8005–8014, doi:10.1039/b905289e, 2009.

Kroll, J. H., Donahue, N. M., Jimenez, J. L., Kessler, S. H., Canagaratna, M. R., Wilson, K. R., Altieri, K. E., Mazzoleni, L. R., Wozniak, A. S., Bluhm, H., Mysak, E. R., Smith, J. D., Kolb, C. E., and Worsnop, D. R.: Carbon oxidation state as a metric for describing the chemistry of atmospheric organic aerosol, Nature Chemistry, 3, 133–139, doi:10.1038/nchem.948, 2011.

Kuwata, M., Zorn, S. R., and Martin, S. T.: Using elemental ratios to predict the density of organic material composed of carbon, hydrogen, and oxygen, Environ. Sci. Technol., 46, 787–794, doi:10.1021/es202525q, 2011.

Lambe, A. T., Chhabra, P. S., Onasch, T. B., Brune, W. H., Hunter, J. F., Kroll, J. H., Cummings, M. J., Brogan, J. F., Parmar, Y., Worsnop, D. R., Kolb, C. E., and Davidovits, P.: Effect of oxidant concentration, exposure time, and seed particles on secondary organic aerosol chemical composition and yield, Atmos. Chem. Phys., 15, 3063–3075, doi:10.5194/acp-15-3063-2015, 2015.

Li, L., Tang, P., Nakao, S., and Cocker III, D. R..: Impact of Molecular Structure on Secondary Organic Aerosol Formation from Aromatic Hydrocarbon Photooxidation under Low NO_x Conditions, Atmos. Chem. Phys. Discuss., in review, 2015.

Liggio, J., Li, S.-M., McLaren, R.: Heterogeneous reactions of glyoxal on particulate matter: Identification of acetals and sulfate esters, Environ. Sci. Technol., 39, 1532–1541, doi:10.1021/es048375y, 2015a.

Liggio, J., Li, S.-M., McLaren, R.: Reactive uptake of glyoxal by particulate matter, J. Geophys. Res.-Atmos., 110, D10304, doi:10.1029/2004JD005113, 2015b.

Lim, Y. B. and Ziemann, P. J.: Effects of molecular structure on aerosol yields from OH radical-initiated reactions of linear, branched, and cyclic alkanes in the presence of NO_x, Environ. Sci. Technol., 43, 2328–2334, doi:10.1021/es803389s, 2009a.

Lockhart, J., Blitz, M., Heard, D., Seakins, P., and Shannon, R.: Kinetic study of the OH[+] glyoxal reaction: experimental evidence and quantification of direct OH recycling, J. Phys. Chem. A., 117, 11027–11037, doi:10.1021/jp4076806, 2013.

Loza, C. L., Chhabra, P. S., Yee, L. D., Craven, J. S., Flagan, R. C., and Seinfeld, J. H.: Chemical aging of *m*-xylene secondary organic aerosol: laboratory chamber study, Atmos. Chem. Phys., 12, 151–167, doi:10.5194/acp-12-151-2012, 2012.

Malloy, Q. G., Nakao, S., Qi, L., Austin, R., Stothers, C., Hagino, H., and Cocker III, D. R.: Real-time aerosol density determination utilizing a modified scanning mobility particle sizer – aerosol particle mass analyzer system, Aerosol Sci. Tech., 43, 673–678, doi:10.1080/02786820902832960, 2009.

Martín-Reviejo, M. and Wirtz, K.: Is benzene a precursor for secondary organic aerosol?, Environ. Sci. Technol., 39, 1045–1054, doi:10.1021/es049802a, 2005.

Matsunaga, A., Docherty, K. S., Lim, Y. B., and Ziemann, P. J.: Composition and yields of secondary organic aerosol formed from OH radical-initiated reactions of linear alkenes in the presence of NO_x: Modeling and measurements, Atmos. Environ., 43, 1349–1357, doi:10.1016/j.atmosenv.2008.12.004, 2009.

McLafferty, F. W. and Tureček, F.: Interpretation of Mass Spectra, Univ. Science Books, Sausalito, CA, USA, 1993.

Nakao, S., Clark, C., Tang, P., Sato, K., and Cocker III, D.: Secondary organic aerosol formation from phenolic compounds in the absence of NO_x, Atmos. Chem. Phys., 11, 10649–10660, doi:10.5194/acp-11-10649-2011, 2011.

Nakao, S., Liu, Y., Tang, P., Chen, C.-L., Zhang, J., and Cocker III, D. R.: Chamber studies of SOA formation from aromatic hydrocarbons: observation of limited glyoxal uptake, Atmos. Chem. Phys., 12, 3927–3937, doi:10.5194/acp-12-3927-2012, 2012.

Nakao, S., Tang, P., Tang, X., Clark, C. H., Qi, L., Seo, E., Asa-Awuku, A., and Cocker III, D.: Density and elemental ratios of secondary organic aerosol: Application of a density prediction method, Atmos. Environ., 68, 273–277,doi:10.1016/j.atmosenv.2012.11.006, 2013.

Ng, N. L., Kroll, J. H., Chan, A. W. H., Chhabra, P. S., Flagan, R. C., and Seinfeld, J. H.: Secondary organic aerosol formation from *m*-xylene, toluene, and benzene, Atmos. Chem. Phys., 7, 3909–3922, doi:10.5194/acp-7-3909-2007, 2007.

Ng, N. L., Canagaratna, M. R., Zhang, Q., Jimenez, J. L., Tian, J., Ulbrich, I. M., Kroll, J. H., Docherty, K. S., Chhabra, P. S., Bahreini, R., Murphy, S. M., Seinfeld, J. H., Hildebrandt, L., Donahue, N. M., DeCarlo, P. F., Lanz, V. A., Prévôt, A. S. H., Dinar, E., Rudich, Y., and

ACPD
15, 31153–31196, 2015

Worsnop, D. R.: Organic aerosol components observed in Northern Hemispheric datasets from Aerosol Mass Spectrometry, Atmos. Chem. Phys., 10, 4625–4641, doi:10.5194/acp-10-4625-2010, 2010.

Ng, N. L., Canagaratna, M. R., Jimenez, J. L., Chhabra, P. S., Seinfeld, J. H., and Worsnop, D. R.: Changes in organic aerosol composition with aging inferred from aerosol mass spectra, Atmos. Chem. Phys., 11, 6465–6474, doi:10.5194/acp-11-6465-2011, 2011.

Noziere, B., Dziedzic, P., and Córdova, A.: Products and kinetics of the liquid-phase reaction of glyoxal catalyzed by ammonium ions (NH_4^+), J. Phys. Chem. A., 113, 231–237, doi:10.1021/jp8078293, 2008.

Odum, J. R., Hoffmann, T., Bowman, F., Collins, D., Flagan, R. C., and Seinfeld, J. H.: Gas/particle partitioning and secondary organic aerosol yields, Environ. Sci. Technol., 30, 2580–2585, doi:10.1021/es950943+, 1996.

Odum, J. R., Jungkamp, T., Griffin, R., Flagan, R. C., and Seinfeld, J. H.: The atmospheric aerosol-forming potential of whole gasoline vapor, Science, 276, 96–99, doi:10.1126/science.276.5309.96, 1997a.

Odum, J. R., Jungkamp, T., Griffin, R. J., Forstner, H., Flagan, R. C., and Seinfeld, J. H.: Aromatics, reformulated gasoline, and atmospheric organic aerosol formation, Environ. Sci. Technol., 31, 1890–1897, doi:10.1021/es960535l, 1997b.

Pang, Y., Turpin, B., and Gundel, L.: On the importance of organic oxygen for understanding organic aerosol particles, Aerosol Sci. Tech., 40, 128–133, doi:10.1080/02786820500423790, 2006.

Pankow, J. F. and Asher, W. E.: SIMPOL.1: a simple group contribution method for predicting vapor pressures and enthalpies of vaporization of multifunctional organic compounds, Atmos. Chem. Phys., 8, 2773–2796, doi:10.5194/acp-8-2773-2008, 2008.

Pfaffenberger, L., Barmet, P., Slowik, J. G., Praplan, A. P., Dommen, J., Prévôt, A. S. H., and Baltensperger, U.: The link between organic aerosol mass loading and degree of oxygenation: an α-pinene photooxidation study, Atmos. Chem. Phys., 13, 6493–6506, doi:10.5194/acp-13-6493-2013, 2013.

Plum, C. N., Sanhueza, E., Atkinson, R., Carter, W. P., and Pitts, J. N.: Hydroxyl radical rate constants and photolysis rates of alpha-dicarbonyls, Environ. Sci. Technol., 17, 479–484, doi:10.1021/es00114a008, 1983.

ACPD
15, 31153–31196, 2015

Qi, L., Nakao, S., Malloy, Q., Warren, B., and Cocker III, D. R.: Can secondary organic aerosol formed in an atmospheric simulation chamber continuously age?, Atmos. Environ., 44, 2990–2996, doi:10.1016/j.atmosenv.2010.05.020, 2010a.
Qi, L., Nakao, S., Tang, P., and Cocker III, D. R.: Temperature effect on physical and chemical properties of secondary organic aerosol from *m*-xylene photooxidation, Atmos. Chem. Phys., 10, 3847–3854, doi:10.5194/acp-10-3847-2010, 2010b.
Rader, D. J. and McMurry, P. H.: Application of the tandem differential mobility analyzer to studies of droplet growth or evaporation, J. Aerosol. Sci., 17, 771–787, doi:10.1016/0021-8502(86)90031-5, 1986.
Salo, K., Hallquist, M., Jonsson, Å. M., Saathoff, H., Naumann, K.-H., Spindler, C., Tillmann, R., Fuchs, H., Bohn, B., Rubach, F., Mentel, Th. F., Müller, L., Reinnig, M., Hoffmann, T., and Donahue, N. M.: Volatility of secondary organic aerosol during OH radical induced ageing, Atmos. Chem. Phys., 11, 11055–11067, doi:10.5194/acp-11-11055-2011, 2011.
Salter, R. J., Blitz, M. A., Heard, D. E., Kovács, T., Pilling, M. J., Rickard, A. R., and Seakins, P. W.: Quantum yields for the photolysis of glyoxal below 350 nm and parameterisations for its photolysis rate in the troposphere, Phys. Chem. Chem. Phys., 15, 4984–4994, doi:10.1039/c3cp43597k, 2013.
Sato, K., Hatakeyama, S., and Imamura, T.: Secondary organic aerosol formation during the photooxidation of toluene: NO_x dependence of chemical composition, J. Phys. Chem. A., 111, 9796–9808, doi:10.1021/jp071419f, 2007.
Sato, K., Takami, A., Isozaki, T., Hikida, T., Shimono, A., and Imamura, T.: 2010. Mass spectrometric study of secondary organic aerosol formed from the photo-oxidation of aromatic hydrocarbons, Atmos. Environ., 44, 1080–1087, doi:10.1016/j.atmosenv.2009.12.013, 2010.
Sato, K., Takami, A., Kato, Y., Seta, T., Fujitani, Y., Hikida, T., Shimono, A., and Imamura, T.: AMS and LC / MS analyses of SOA from the photooxidation of benzene and 1,3,5-trimethylbenzene in the presence of NO_x: effects of chemical structure on SOA aging, Atmos. Chem. Phys., 12, 4667–4682, doi:10.5194/acp-12-4667-2012, 2012.
Shilling, J. E., Chen, Q., King, S. M., Rosenoern, T., Kroll, J. H., Worsnop, D. R., DeCarlo, P. F., Aiken, A. C., Sueper, D., Jimenez, J. L., and Martin, S. T.: Loading-dependent elemental composition of α-pinene SOA particles, Atmos. Chem. Phys., 9, 771–782, doi:10.5194/acp-9-771-2009, 2009.

ACPD
15, 31153–31196, 2015

Role of methyl group number on SOA formation

L. Li et al.

Title Page
Abstract Introduction
Conclusions References
Tables Figures
◀◀ ▶▶
◀ ▶
Back Close
Full Screen / Esc
Printer-friendly Version
Interactive Discussion

Singh, H. B., Salas, L. J., Cantrell, B. K., and Redmond, R. M.: Distribution of aromatic hydrocarbons in the ambient air, Atmos. Environ., 19, 1911–1919, doi:10.1016/0004-6981(85)90017-4, 1985.
Singh, H. B., Salas, L., Viezee, W., Sitton, B., and Ferek, R.: 1992. Measurement of volatile organic chemicals at selected sites in California, Atmos. Environ. A-Gen., 26, 2929–2946, doi:10.1016/0960-1686(92)90285-S, 1992.
Song, C., Na, K., and Cocker III, D. R.: Impact of the hydrocarbon to NO_x ratio on secondary organic aerosol formation, Environ. Sci. Technol., 39, 3143–3149, doi:10.1021/es0493244, 2005.
Takegawa, N., Miyakawa, T., Kawamura, K., and Kondo, Y.: Contribution of selected dicarboxylic and ω-oxocarboxylic acids in ambient aerosol to the m/z 44 signal of an Aerodyne aerosol mass spectrometer, Aerosol Sci. Tech., 41, 418–437, doi:10.1080/02786820701203215, 2007.
Takekawa, H., Minoura, H., and Yamazaki, S.: Temperature dependence of secondary organic aerosol formation by photo-oxidation of hydrocarbons, Atmos. Environ., 37, 3413–3424, doi:10.1016/S1352-2310(03)00359-5, 2003.
Tkacik, D. S., Presto, A. A., Donahue, N. M., and Robinson, A. L.: Secondary organic aerosol formation from intermediate-volatility organic compounds: cyclic, linear, and branched alkanes, Environ. Sci. Technol., 46, 8773–8781, doi:10.1021/es301112c, 2012.
Tritscher, T., Dommen, J., DeCarlo, P. F., Gysel, M., Barmet, P. B., Praplan, A. P., Weingartner, E., Prévôt, A. S. H., Riipinen, I., Donahue, N. M., and Baltensperger, U.: Volatility and hygroscopicity of aging secondary organic aerosol in a smog chamber, Atmos. Chem. Phys., 11, 11477–11496, doi:10.5194/acp-11-11477-2011, 2011.
Võ, U.-U. T., and Morris, M. P.: Nonvolatile, semivolatile, or volatile: Redefining volatile for volatile organic compounds, JAPCA J. Air Waste Ma., 64, 661–669, doi:10.1080/10962247.2013.873746, 2014.
Wyche, K. P., Monks, P. S., Ellis, A. M., Cordell, R. L., Parker, A. E., Whyte, C., Metzger, A., Dommen, J., Duplissy, J., Prevot, A. S. H., Baltensperger, U., Rickard, A. R., and Wulfert, F.: Gas phase precursors to anthropogenic secondary organic aerosol: detailed observations of 1,3,5-trimethylbenzene photooxidation, Atmos. Chem. Phys., 9, 635–665, doi:10.5194/acp-9-635-2009, 2009.
Xiang, B., Zhu, L., and Tang, Y.: Photolysis of 4-Oxo-2-pentenal in the 190–460 nm Region, J. Phys. Chem. A., 111, 9025–9033, doi:10.1021/jp0739972, 2007.

Yu, J., Jeffries, H. E., and Sexton, K. G.: Atmospheric photooxidation of alkylbenzenes – I. Carbonyl product analyses, Atmos. Environ., 31, 2261–2280, doi:10.1016/S1352-2310(97)00011-3, 1997.
Yu, L., Smith, J., Laskin, A., Anastasio, C., Laskin, J., and Zhang, Q.: Chemical characterization of SOA formed from aqueous-phase reactions of phenols with the triplet excited state of carbonyl and hydroxyl radical, Atmos. Chem. Phys., 14, 13801–13816, doi:10.5194/acp-14-13801-2014, 2014.
Zhang, Q., Alfarra, M. R., Worsnop, D. R., Allan, J. D., Coe, H., Canagaratna, M. R., and Jimenez, J. L.: Deconvolution and quantification of hydrocarbon-like and oxygenated organic aerosols based on aerosol mass spectrometry, Environ. Sci. Technol., 39, 4938–4952, doi:10.1021/es048568l, 2005.
Ziemann, P.: Effects of molecular structure on the chemistry of aerosol formation from the OH-radical-initiated oxidation of alkanes and alkenes, Int. Rev. Phys. Chem., 30, 161–195, doi:10.1080/0144235X.2010.550728, 2011.

ACPD
15, 31153–31196, 2015

Table 1. Experiment conditions[d].

Precursor	ID	HC/NO[a]	NO[b]	HC[b]	ΔHC[c]	M_0^c	Yield
Benzene	1223 A	98.1	59.5	972	398	139	0.35
	1223B	49.3	119	979	453	105	0.23
	1236 A	104	53.6	928	407	106	0.26
	1236B	36.4	154	938	450	34.9	0.08
	1237 A	62.7	41.6	435	266	45.9	0.17
	1237B	129	21.1	453	253	51.4	0.20
	1618 A	102	35.4	603	354	46.3	0.13
Toluene	1101 A	29.0	19.2	79.7	206	30.1	0.15
	1101B	58.8	9.40	78.8	176	25.1	0.14
	1102 A	12.2	43.3	75.7	223	21.8	0.10
	1102B	17.5	33.0	82.5	238	22.2	0.09
	1106 A	13.2	20.1	38.0	126	9.80	0.08
	1106B	24.4	10.6	36.9	111	12.4	0.11
	1468 A	26.1	64.1	239	667	130	0.20
	1468B	26.5	63.0	238	671	127	0.19
m-Xylene	1191 A	12.6	52.2	82.1	298	15.2	0.05
	1191B	14.6	45.7	83.6	340	14.6	0.04
	1193 A	15.5	36.8	71.1	239	13.6	0.06
	1193B	15.2	36.5	69.5	236	11.2	0.05
	1191 A	12.6	52.2	82.1	298	15.2	0.05
	1191B	14.6	45.7	83.6	340	14.6	0.04
	1516 A	27.8	26.7	92.9	357	48.7	0.14
	1950 A	14.1	45.5	80.0	327	26.3	0.08
	1950B	14.6	45.9	83.6	345	28.7	0.08

ACPD
15, 31153–31196, 2015

Role of methyl group number on SOA formation

L. Li et al.

Table 1. Continued.

Precursor	ID	HC/NO[a]	NO[b]	HC[b]	ΔHC^c	M_0^c	Yield
1,2,4-Trimethylbenzene	1117 A	69.8	10.3	80.0	335	16.8	0.05
	1117B	34.8	20.7	80.0	368	18.2	0.05
	1119 A	14.1	49.8	78.0	385	19.6	0.05
	1119B	17.1	41.6	79.0	390	25.5	0.07
	1123 A	71.0	10.1	80.0	300	11.2	0.04
	1123B	32.6	22.1	80.0	345	15.4	0.05
	1126 A	69.3	10.1	77.5	286	12.6	0.04
	1126B	28.1	24.3	75.9	333	15.4	0.05
	1129B	24.2	15.6	42.0	201	5.60	0.03
1,2,4,5-Tetramethylbenzene	1531 A	72.0	25.0	180	752	17.9	0.02
	1603 A	109	11.2	122	469	3.12	0.01
	1603B	110	11.1	123	464	2.54	0.01
	2085 A	60.6	33.4	202	862	29.2	0.03
	2085B	136	12.9	175	502	8.20	0.02
Pentamethylbenzene	1521 A	68.8	23.5	147	893	32.7	0.04
	1627 A	77.9	20.0	142	769	20.6	0.03
	1627B	26.6	50.0	121	719	24.8	0.03
Hexamethylbenzene	1557 A	72.0	28.0	168	999	23.4	0.02
	2083 A	78.4	11.6	76.0	442	15.2	0.03
	2083B	41.3	22.0	76.0	483	14.0	0.03

Note: [a] Unit of HC/NO are ppbC : ppb; [b] unit of NO and HC are ppb; [c] unit of ΔHC and M_0 are $\mu g\,m^{-3}$, M_0 is a wall loss and density corrected particle mass concentration; [d] only newly added data are listed here and published data are listed in Table S2.

ACPD
15, 31153–31196, 2015

Table 2. Two product yield curve fitting parameters.

Yield curve	α_1	$K_{om,1}$ ($m^3\,\mu g^{-1}$)	α_2	$K_{om,2}$ ($m^3\,\mu g^{-1}$)
Benzene	0.082	0.017	0.617	0.005
Toluene	0.185	0.080	0.074	0.005
m-Xylene	0.148	0.047	0.079	0.005
1,2,4-Trimethylbenzene	0.099	0.047	0.079	0.005
C_{10+}	0.048	0.047	0.065	0.005

ACPD
15, 31153–31196, 2015

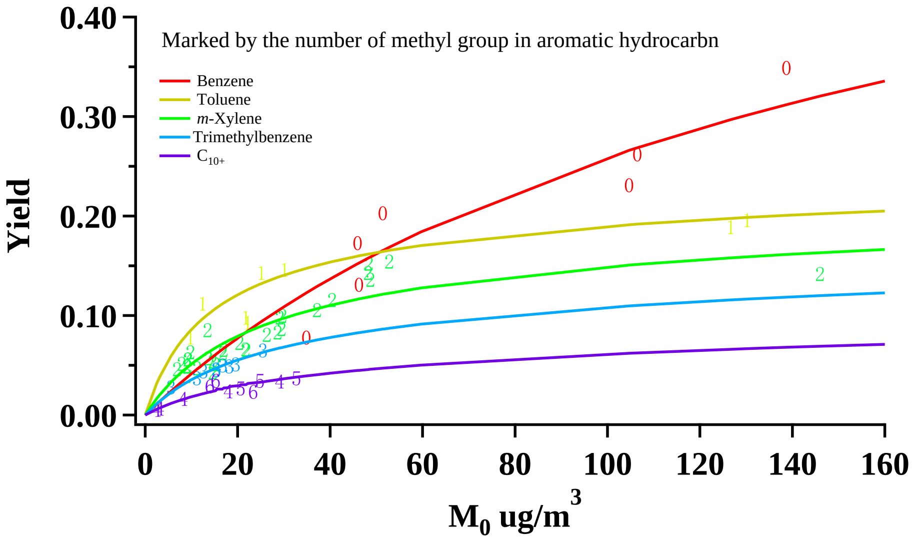

Figure 1. Aromatic SOA yields as a function of M_0. Note: Song et al. (2005) *m*-xylene data are also included.

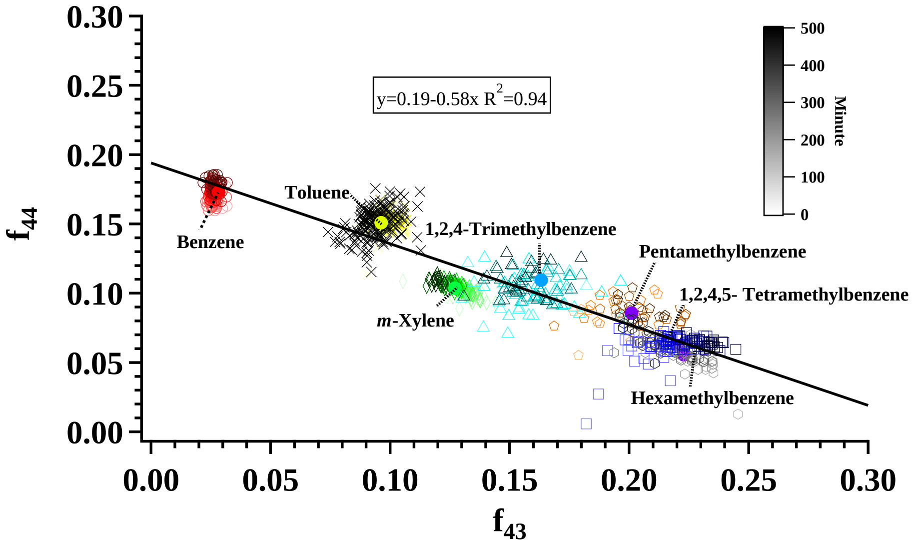

Figure 2. f_{44} and f_{43} evolution in SOA formed from photooxidation of different aromatic hydrocarbons under low NO_x (Benzene 1223 A; Toluene 1468 A; *m*-Xylene 1950 A; 1,2,4-Trimethylbenzene 1119 A; 1,2,4,5-Tetramethylbenzene 2085 A; Pentamethylbenzene 1627 A; Hexamethylbenzene 2083 A; colored solid circle markers represent the location of average f_{44} and f_{43} value during photooxidation).

ACPD
15, 31153–31196, 2015

Role of methyl group number on SOA formation

L. Li et al.

Title Page
Abstract | Introduction
Conclusions | References
Tables | Figures
◀I | ▶I
◀ | ▶
Back | Close
Full Screen / Esc
Printer-friendly Version
Interactive Discussion

ACPD
15, 31153–31196, 2015

Role of methyl group number on SOA formation

L. Li et al.

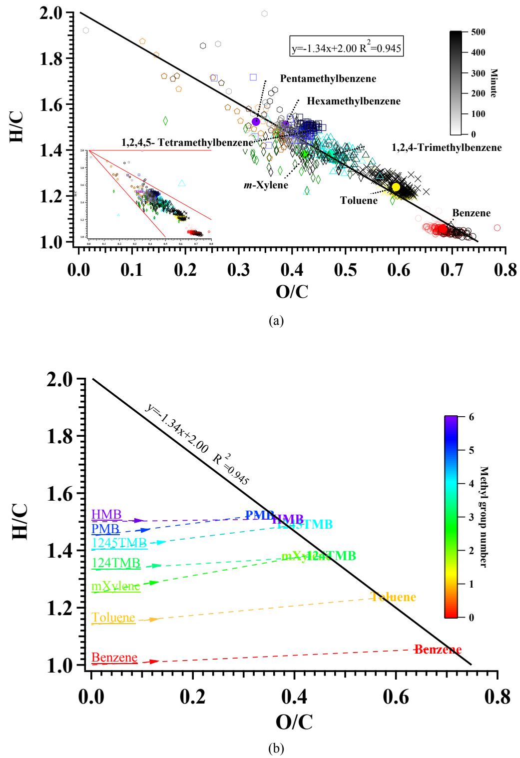

Figure 3. (a) H/C and O/C evolution; the inset graph shows the measured values relative to the classic triangle plot (Ng et al., 2010). **(b)** Average H/C and O/C in SOA formed from aromatic hydrocarbon photooxidation under low NO_x (Benzene 1223 A; Toluene 1468 A; *m*-Xylene 1191 A; 1,2,4-Trimethylbenzene 1119 A; 1,2,4,5-Tetramethylbenzene 2085 A; Pentamethylbenzene 1627 A; Hexamethylbenzene 2083 A).

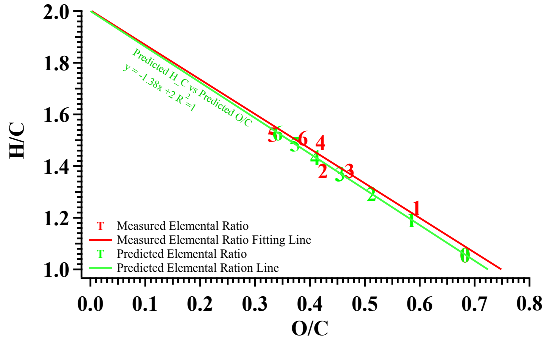

(a)

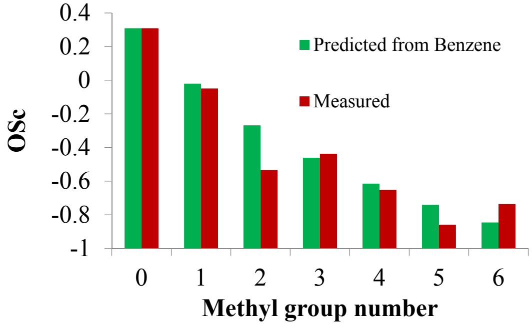

(b)

Figure 4. Comparison of predicted and measured O/C **(a)**, H/C **(a)** and oxidation state (OSc) **(b)** in SOA formation from aromatic hydrocarbon photooxidation under low NO_x (Benzene 1223 A; Toluene 1468 A; m-Xylene 1191 A; 1, 2, 4-Trimethylbenzene 1119 A; 1,2,4,5-Tetramethylbenzene 1306 A; Pentamethylbenzene 1627 A; Hexamethylbenzene 1557 A).

ACPD
15, 31153–31196, 2015

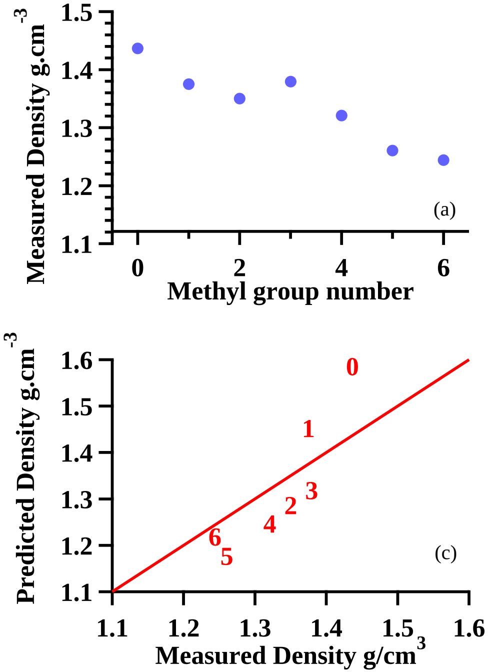

Figure 5. Relationship between **(a)** SOA density and methyl group number; **(b)** SOA density and O/C; **(c)** predicted and measured density from aromatic hydrocarbon photooxidation under low NO_x (number mark represents number of methyl groups on aromatic hydrocarbon ring).

ACPD
15, 31153–31196, 2015

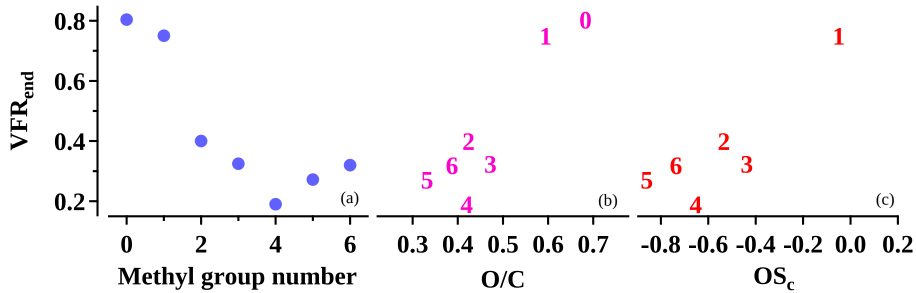

Figure 6. Relationship between **(a)** SOA volatility and methyl group number; **(b)** SOA volatility and O/C; **(c)** SOA volatility and oxidation state (OS_c) from aromatic hydrocarbon photooxidation under low NO_x (number mark represents number of methyl groups on aromatic hydrocarbon ring).

ACPD
15, 31153–31196, 2015

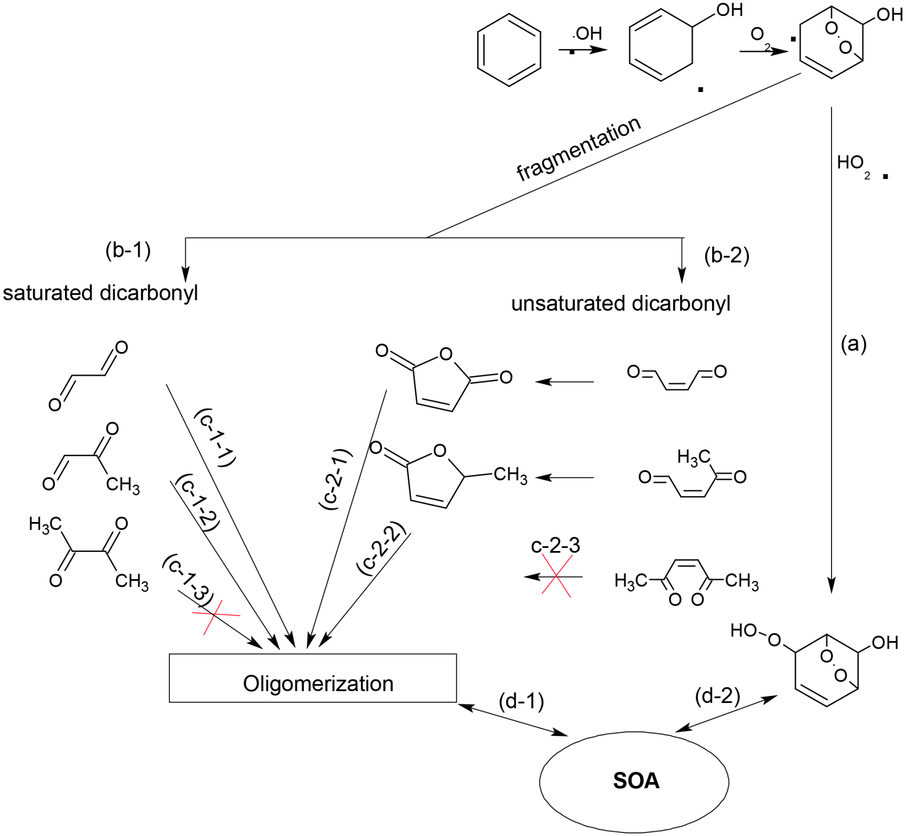

Figure 7. Aromatic hydrocarbon oxidation pathways related to SOA formation (benzene shown as an example).

ACPD
15, 31153–31196, 2015

Role of methyl group number on SOA formation

L. Li et al.

Title Page
Abstract | Introduction
Conclusions | References
Tables | Figures
◀| |▶
◀ ▶
Back | Close
Full Screen / Esc
Printer-friendly Version
Interactive Discussion

$$\text{Aromatic Hydrocarbon} + \text{OH} \rightarrow S_1^{g} \rightarrow S_2^{g} \rightarrow S_3^{g}$$

$$S_1^{g} \rightleftarrows S_1^{p} \qquad S_3^{g} \rightleftarrows S_3^{p}$$

Figure 8. Kinetic scheme for SOA formation from aromatic hydrocarbon.

ACPD
15, 31153–31196, 2015